Article:
Azizi, S, Liu, G, Dobakhshari, AS et al. (2020) Wide-Area Backup Protection Against Asymmetrical Faults Using Available Phasor Measurements. IEEE Transactions on Power Delivery, 45 (4). pp. 2032-2039. ISSN: 0885-8977

https://doi.org/10.1109/TPWRD.2019.2960352

Wide-Area Backup Protection against Asymmetrical Faults Using Available Phasor Measurements

Sadegh Azizi, *Senior Member*, *IEEE*, Gaoyuan Liu, *Student Member*, *IEEE*, Ahmad Salehi Dobakhshari, *Member*, *IEEE*, and Vladimir Terzija, *Fellow*, *IEEE*

***Abstract*— This paper proposes a robust and computationally efficient wide-area backup protection (WABP) scheme against asymmetrical faults on transmission systems using available synchronized/unsynchronized phasor measurements. Based on the Substitution Theorem, the proposed scheme replaces the faulted line with two suitable current sources. This results in a linear system of equations for WABP, with no need of full system observability by measurement devices. The identification of the faulted line is attributed to the sum of squared residuals (*SoSR*) of the developed system of equations. To preserve accuracy, the scheme limits the calculations to the assessment of the negative-sequence circuit of the gird. Relevant practical aspects that have not been properly addressed in the literature, namely the non-simultaneous opening of circuit breakers (CBs) and their single-pole tripping for single-phase to ground faults are investigated. The linearity of the formulations derived removes concerns over convergence speed and potential time-synchronization challenges. The proposed scheme is able to identify the faulted line and retain this capability for hundreds of milliseconds following the fault inception. More than 20,000 simulations conducted on the IEEE 39-bus test system verify the effectiveness of the proposed WABP scheme.**

***Index Terms*— Least squares method, Sequence circuits, Time-synchronization errors, Wide area backup protection.**

I. Introduction

BACKUP protection is an indispensable element of power system protection, guaranteeing continuous operation of the system in the event of failure of primary protection [1, 2]. Asymmetrical faults are the most frequent type of short-circuit faults on transmission systems [3, 4]. The reliability of backup protection against asymmetrical faults is of the utmost importance as its misoperation or malfunction might cause unstoppable cascading events and even lead to catastrophic power system blackouts [5-7].

Inaccurate measurements of voltage and current phasors during short-circuit faults in the system are amongst the main root causes of failures of conventional local protection schemes [8-10]. Erroneous phasor measurements upon a fault essentially result from transient responses of instrument transformers in the proximity of the fault location [1, 2]. Wide-area monitoring systems (WAMS) can offer a more effective backup protection compared to local protection schemes, because of their capability of capturing a reliable set of phasor measurements and having a broader view of processes across the grid [11]. Wide-area backup protection (WABP) is defined as the application of phasors provided by PMUs, digital protective relays and intelligent electronic devices (IEDs) to inferring and disconnecting the faulted line when primary protection fails to do so [12].

WABP is expected to correctly pinpoint the faulted line and retain this capability for a sufficiently long period of time, *i.e.*, hundreds of milliseconds following the fault inception. This is necessary for coordinating local and wide-area backup protections, and also generating appropriate trip commands in the event of circuit breaker (CB) failures. A temporary loss of the time-synchronization signal must not affect the expected functionality of WABP. This implies that a reliable WABP scheme needs to be robust in situations where its input phasors are not time-synchronized. The requirements just described are beyond the capabilities of the existing WABP schemes.

Theoretically, two independent synchrophasors would be sufficient to determine the faulted line and the exact fault distance [13-16]. Nevertheless, many of the existing WABP schemes require special PMU placements in order to be able to cover faults on the entire transmission grid [17-26]. Nonetheless, it is unlikely that system operators place PMUs in the system merely for meeting the requirements of a single functionality [16]. Rather, the availability of communication infrastructure and instrument transformers in substations are the main practical factors determining PMU locations [27]. In addition, single-pole fault clearing is a recommended practice for improving stability of transmission systems following single-phase-to-ground (1-ph-g) faults. Fault type identification is a prerequisite to enable this feature. Nonetheless, existing WABP schemes have not dealt with this requirement so far, assuming that fault clearing will be always carried out three-pole irrespective of the fault type.

Modelling generators in the positive-sequence circuit as a fixed impedance behind a constant voltage source reduces the computational burden of WABP, at the expense of neglecting time-variance of generator impedances, their rotor saliency and automatic voltage regulator effects [3]. In the zero- and negative-sequence circuits, synchronous machines are simply represented by their impedances to the flow of zero- and negative-sequence currents, respectively, which are time-invariant contrary to their positive-sequence counterpart [3]. Considering the uncertainty involved in calculating zero

Paper no. TPWRD-00769-2019. *(Corresponding author: Ahmad Salehi Dobakhshari.)*

Sadegh Azizi is with the School of Electronic and Electrical Engineering, University of Leeds, Leeds LS2 9JT, UK (e-mail: s.azizi@leeds.ac.uk).

Gaoyuan Liu and Vladimir Terzija are with the School of Electrical and Electronic Engineering, University of Manchester, Manchester M13 9PL, UK (e-mail: gaoyuan.liu@manchester.ac.uk; vladimir.terzija@manchester.ac.uk).

Ahmad Salehi Dobakhshari is with the Faculty of Engineering, University of Guilan, Rasht 4199613776, Iran (e-mail: salehi_ahmad@guilan.ac.ir).

sequence impedances of transmission lines [4], the negative-sequence circuit is the most suitable circuit for individual analysis of asymmetrical faults.

This paper proposes a WABP scheme for deployment in transmission systems. The scheme is capable of identifying the faulted line and retaining this capability for hundreds of milliseconds following the inception of an asymmetrical fault. This facilitates establishing a two-way communication between the wide-area and local protection systems until the fault is cleared. Such a communication is necessary to properly respond to possible CB failures hindering the disconnection of the faulted line. The speed of protection systems is considered quite important contrary to that of offline processes such as fault location [4]. The derivations of the proposed scheme comprise a system of linear equations, which can be solved by the ordinary linear least squares method. This resolves the concerns over computational burden, the success and speed of convergence as well as multiple solutions, typical for existing nonlinear WABP formulations [28].

II. Proposed Wide-Area Backup Protection Scheme

The applications of circuit theorems in facilitating fault studies is explained in this section. These are then used to develop a system of linear equations for WABP by available synchronized/unsynchronized phasor measurements. Finally, the procedure for the identification of the faulted line and fault type before and after the opening of CBs is explained.

A. Application of Circuit Theorems in Fault Studies

Let us consider a circuit with N nodes with the bus impedance matrix $\boldsymbol{Z}$. Assume the disturbance of interest is a change in the values of nodal current injections in the circuit. Let $\Delta\boldsymbol{V}$ and $\Delta\boldsymbol{I}$ denote the vectors of superimposed node voltages and superimposed nodal currents, respectively. Based on the *Substitution Theorem*, one can write [29]

$$\Delta\boldsymbol{V} = \boldsymbol{Z}\Delta\boldsymbol{I} \tag{1}$$

The Δ symbol refers to the fact that superimposed node voltages and nodal currents are equal to the differences between their corresponding quantities before and after the disturbance. If ΔI_j refers to the superimposed nodal current injection at node j, the superimposed voltage at the node i is obtained from

$$\Delta V_i = \sum_{j=1}^{N} Z_{i,j}\Delta I_j, \qquad \forall 1 \le i \le N \tag{2}$$

where $Z_{i,j}$ is the element in the i-th row and j-th column of the bus impedance matrix.

Let ΔJ^s_{uv} denote the superimposed current of the sending-end a non-faulted line u-v in the power system. Here, s is used to refer to the corresponding sequence circuit and takes a value of "*0*", "*+*" or "*–*" for the zero-, positive- and negative-sequence circuits, respectively. It can be easily shown that

$$\Delta J^s_{uv} = \sum_{q=1}^{N} C^s_{uv,q}\Delta I^s_q \tag{3}$$

where the derivation of $C^s_{uv,q}$ is detailed in [9].

B. A Linear System of Equations for WABP

In this subsection, the WABP problem is first formulated based on synchrophasor inputs. In the next step, a solution based on unsynchronized phasor inputs is proposed enabling a more flexible and robust WABP.

1) *Application of synchrophasor measurements:* In order to use the superimposed circuit technique, the faulted line in the negative-sequence circuit is substituted by two current sources injecting the same amount of negative-sequence currents as the line does. Let us assume that line *i-j* is the faulted line and that $\boldsymbol{Z}^-$ denotes the bus impedance matrix of the negative-sequence circuit when line *i-j* is disconnected from the grid. Based on (2), the superimposed voltage measured by a PMU at an arbitrary bus q satisfies the following equation

$$\Delta V_q^{-,meas} = Z^-_{q,i}\Delta I^-_i + Z^-_{q,j}\Delta I^-_j + e^V_q \tag{4}$$

where the superscript "*meas*" refers to measured quantities, and e^V_q denotes the associated measurement error.

As stated, ΔJ^-_{uv} denotes the superimposed negative-sequence current of the sending-end of a non-faulted line u-v. As the superimposed negative-sequence circuit includes only two current sources, (3) can be simplified to

$$\Delta J_{uv}^{-,meas} = C^-_{uv,i}\Delta I^-_i + C^-_{uv,j}\Delta I^-_j + e^I_{uv} \tag{5}$$

where e^I_{uv} stands for the associated measurement error.

On the other hand, ΔJ^-_i and ΔJ^-_j are the superimposed sending- and receiving-end currents of the faulted line, respectively. Subject to measuring these two current phasors by PMUs, the equations below can be also established

$$\begin{cases} \Delta J_i^{-,meas} = -\Delta I^-_i + e^I_{ij} \\ \Delta J_j^{-,meas} = -\Delta I^-_j + e^I_{ji} \end{cases} \tag{6}$$

where the negative signs on the right-hand side of the equations result from the conventions assumed for the direction of nodal injections and transmission line currents.

Let us assume PMUs provide p voltage and current measurements from across the grid. Writing equations corresponding to these measurements, a system of linear equations as below can be obtained

$$\boldsymbol{m}_{p\times 1} = \boldsymbol{H}_{p\times 2}\boldsymbol{x}_{2\times 1} + \boldsymbol{\varepsilon}_{p\times 1}\,. \tag{7}$$

where $\boldsymbol{m}$, $\boldsymbol{H}$ and $\boldsymbol{\varepsilon}$ are the measurement vector, coefficient matrix and error vector, respectively. Further, $\boldsymbol{x}$ is the vector of unknown current sources replaced for the faulted line, as detailed below

$$\boldsymbol{x} = \begin{bmatrix} \Delta I^-_i & \Delta I^-_j \end{bmatrix}^T \tag{8}$$

The overdetermined system of linear equations (7) can be readily solved using the linear least-squares method as follows

$$\hat{\boldsymbol{x}} = \left(\boldsymbol{H}^*\boldsymbol{H}\right)^{-1}\boldsymbol{H}^*\boldsymbol{m} \tag{9}$$

where the asterisk on $\boldsymbol{H}$ refers to the conjugate transpose of that matrix. The vector $\hat{\boldsymbol{x}}$ contains estimates that may not be exactly equal to their corresponding true values, as a result of measurement errors incurred in practice.

2) Application of unsynchronized phasor measurements: Voltage and current phasors calculated by a PMU or IED at a substation will be all synchronized to the local time reference of that device, which might or might not be aligned with a common time reference in the whole grid. In practice, the time drift of locally-measured phasors caused by the loss of the time synchronisation signal and/or essentially the use of a local time reference can be readily limited to 1.5 μs within a 1 sec period [30]. Hence, the phase-angles of pre- and post-fault phasors associated with the same substation remain extremely accurate with respect to each other within the time frame of interest to WABP. Therefore, the main challenge of WABP with unsynchronized inputs is to align the local reference of each device to a common universal time reference [28, 30].

Let us assume that PMUs are installed at buses 1 to *n*. Our focus here is on situations in which the time-synchronization between measured phasors is lost. To be able to use the Phasor Method, all voltage and current signals should be expressed with respect to a common time reference [28]. Without loss of generality, the time reference of the PMU at bus 1 is taken as the common reference for all measurements. Then, phasors provided by PMUs at buses 2 to n are multiplied by the unknown synchronization operators $e^{j\delta_2}, e^{j\delta_3}, \ldots, e^{j\delta_n}$, respectively. Let us assume that, for instance, m_1 to m_f denote the phasors provided by PMU_1, and m_{f+1} to m_s denote the phasors provided by PMU_2. Therefore,

$$\boldsymbol{m} = \left[m_1, \ldots, m_f, m_{f+1}e^{j\delta_2}, \ldots, m_s e^{j\delta_2}, \ldots, m_p e^{j\delta_n} \right]^T \quad (10)$$

Inserting the above synchronized measurement vector into (7) makes that system of equations nonlinear in terms of the unknown synchronization angles δ_2, δ_3, …, δ_n. The resulting system of non-linear equations can be iteratively solved, for instance, by the approach presented in [28]. However, iterative solutions are in general subject to convergence failures and/or multiple (suboptimal) solutions. To overcome this type of concerns, the obtained system of equations is innovatively re-formulated as a linear combination of unknown variables and synchronization operators, as shown in (11) at the bottom of this page. This new system of equations can be solved using ordinary linear least squares method. The rest of the WABP process would be exactly the same as the one with synchronized measurements.

Preprocessing is necessary to the proposed scheme similar to other applications of PMUs. For example, the data quality flag in PMU output can be used to exclude the bad PMU data from our calculations [31]. One sample from before and one sample from after the fault inception instant will be enough to calculate the superimposed quantities used in the developed system of equations. It follows that the proposed scheme will function desirably irrespective of the reporting rate of PMUs as long as they are compatible with the corresponding standard [31]. The solvability of the system of equations is not dependent on the availability of any specific single equation. Generally speaking, excluding the equations of a few PMUs whose data have not been received or excluded from the input data set for any reasons, would not impair the functionality of the whole WABP scheme. Utilizing the approach presented by the authors in [9], it is possible to determine the simultaneous loss of which equations together may render the system of equations unsolvable.

C. Identifying the Faulted Line and Fault Type

The system of equations (7) is constructed assuming that the line *i-j* is the faulted line. The sum of squared-residuals (*SoSR*) is the objective function minimized for solving (7) by the least-squares method [9], and can be obtained from

$$SoSR = \left[\boldsymbol{m}\text{-}\boldsymbol{H}\hat{\boldsymbol{x}} \right]^* \left[\boldsymbol{m}\text{-}\boldsymbol{H}\hat{\boldsymbol{x}} \right] \quad (12)$$

As discussed in [13], the *SoSR* of the faulted line is zero whereas that of non-faulted lines is non-zero. Accordingly, (12) should be evaluated for different suspected lines in order to identify the faulted line. Once the faulted line is determined, the superimposed currents calculated from (9) can be put into (4) to obtain the superimposed voltages at the faulted line terminals. Having obtained the superimposed voltage and current phasors at the faulted line terminals, the closed-form expression introduced in [13] can be used to obtain the fault distance.

To improve stability of transmission systems, it may be recommended to open only the faulted phase following 1-ph-g faults [1], [2]. In such a case, the identification of the faulted phase will be of particular interest to WABP. On the other hand, the faulted phase is taken as the reference phase for calculating the symmetrical components in the event of single-phase faults [2]. The non-faulted phase would be taken as the reference phase for double-phase faults [2]. If this is not followed, the phase-angles of symmetrical components obtained will differ with those of true symmetrical components by an integer multiple of 60° [3].

In this paper, phase *A* is always taken as the reference phase, regardless of the fault type. Without loss of generality,

$$\begin{bmatrix} m_1 \\ \vdots \\ m_f \\ 0 \\ \vdots \\ 0 \\ \vdots \\ 0 \end{bmatrix} = \begin{bmatrix} H_{1,i} & H_{1,j} & 0 & \cdots & 0 \\ \vdots & \vdots & \vdots & \ddots & \vdots \\ H_{f,i} & H_{f,j} & 0 & \cdots & 0 \\ H_{f+1,i} & H_{f+1,j} & -m_{f+1} & \cdots & 0 \\ \vdots & \vdots & \vdots & \ddots & \vdots \\ H_{s,i} & H_{s,j} & -m_s & \cdots & 0 \\ \vdots & \vdots & \vdots & \ddots & \vdots \\ H_{p,i} & H_{p,j} & 0 & \cdots & -m_p \end{bmatrix} \begin{bmatrix} \Delta I_i^- \\ \Delta I_j^- \\ e^{j\delta_2} \\ \vdots \\ e^{j\delta_n} \end{bmatrix} + \begin{bmatrix} \varepsilon_1 \\ \vdots \\ \varepsilon_n \end{bmatrix} \quad (11)$$

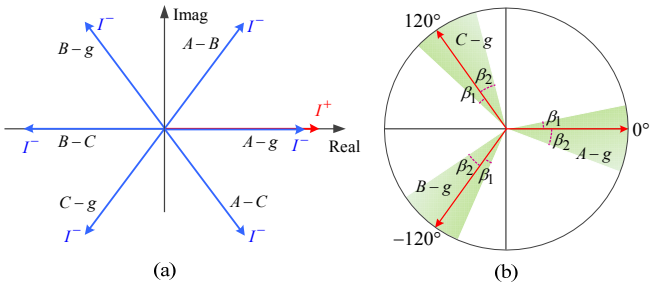

(a) (b)

Fig. 1 (a) Locus of the negative-sequence current for different fault types. (b) Identification of 1-ph-g faults using the phase-angle difference between positive- and negative-sequence currents.

the positive-sequence fault current is then aligned with the real axis of the complex plane. Accordingly, the locus of the negative-sequence fault current will vary depending on the fault type, as shown in Fig. 1(a). The idea here is to use the phase-angle difference between positive- and negative-sequence currents in order to identify 1-ph-g faults. Being denoted by θ, the locus of this phase-angle difference for *A-g*, *B-g* and *C-g* faults are shown in red rays in the unit circle of Fig. 1(b). Accounting for measurement and numerical errors, a clockwise and a counterclockwise uncertainty margins are also appended to each 1-ph-g fault type locus. Based on extensive simulations conducted, β_1 and β_2 are set to 20° and 30°, respectively. Accordingly, the index below is introduced for fault type identification

$$\theta_{ave.} = \frac{1}{l}\sum_{k=1}^{l}\left(\angle\Delta I_k^+ - \angle\Delta I_k^-\right) \tag{13}$$

where l is the number of current phasors. The index $\theta_{ave.}$ for *A-g*, *B-g* and *C-g* faults will lie within the corresponding sector shown in green in the unit circle of Fig. 1(b).

D. Non-Simultaneous Tripping of the Faulted Line

Subsequent to a short-circuit fault on a line, CBs at the line ends will be opened following the reception of a trip command from the corresponding relays. However, the disconnection of the two line-ends may not occur at the same time, *i.e.,* simultaneously. Seeing the fault in different protection zones and/or uncertain CB opening times are the main reasons of such non-simultaneity. It is important for a WABP scheme to be able to distinguish the faulted line even after its single-end disconnection. The single-end disconnection of the faulted line may be accomplished in less than a couple of power frequency cycles following the fault inception. This can be nearly as short as, or even shorter than the data-window length of the phasor estimation method used (*e.g.,* 20 ms). Phasors estimated within that period of time will not be accurate due to inherent transient response of phasor estimation algorithms. Therefore, the WABP scheme may not be able to identify the faulted line by using the inaccurate phasors estimated within such a short period of time.

If the single-end disconnection of the faulted line is three-pole, the fault will be fed only from one end. In this situation, (7) can be still applied to obtain the superimposed current from that opposite line-end. The superimposed current obtained for the disconnected end of the line will be negligible. The same reasoning also applies in cases when CBs open single-pole. The only difference is that the negative-sequence current injected by a single-pole opened CB will not be zero. This will not affect the validity of the proposed system of equations, as will be verified in the simulation section. The reason is that the faulted line is modeled by two current sources at its ends, with no constraint over the amount of currents injected by these sources.

III. Performance Evaluation

The performance of the proposed WABP scheme is evaluated by conducting more than 20,000 simulations on the IEEE 39-bus test system using DIgSILENT PowerFactory. This test system includes 10 generators, 12 power transformers and 34 transmission lines [32]. Buses 3, 5, 8, 11, 14, 16, 19, 23, 25, 27, 29 and 39 are equipped with PMUs to make the system observable [33]. The performance of the proposed scheme is evaluated with both synchronized and unsynchronized measurements. The sensitivity of the proposed scheme to measurement and line parameter errors is studied, afterwards. Comparison with other existing WABP schemes is carried out in the last subsection.

Time-domain voltage and current waveforms recorded during different simulations are filtered using an anti-aliasing Butterworth filter with a cut-off frequency of 400 Hz. Then, they are sampled with a sampling frequency of 2 kHz. To estimate phasors of time-domain waveforms, the discrete Fourier transform (DFT) and a real PMU model are used [34]. When the magnitude of negative- and zero-sequence currents reported by PMUs exceeds a few percent of the positive sequence one (10 % in this study), the proposed scheme will start checking if these variations have resulted from a short-circuit fault. The line corresponding to the minimum *SoSR* calculated is pinpointed as the faulted line. To confirm this, the calculated fault distance on the identified line is also checked to make sure it lies within the acceptable range.

To simplify compliance specification of PMUs, magnitude and angle error bounds are normally combined into a single error quantity referred to as total vector error (TVE) [31]. The TVE is a measure of the difference between the phasor reported by the PMU and the true phasor. The IEEE standard for synchrophasor measurements establishes a criterion of 1% for the TVE. This means the maximum magnitude error is 1% when the error in phase-angle is zero. Besides, the maximum error in phase-angle is 0.573º, which corresponds to a maximum time error of ±31 μs for 50 Hz systems [31]. The performance of the proposed scheme with input phasors having different ranges of TVEs is studied in subsection III-C.

A. WABP using Synchronized Phasor Measurements

In this subsection, the performance of the proposed scheme, its applicability to symmetrical faults, and the process of faulted line identification are studied.

1) General Evaluation of the Proposed WABP Scheme:

To demonstrate the effectiveness of the proposed WABP scheme, different types of asymmetrical faults with fault resistances of 0 Ω, 10 Ω and 50 Ω are applied at different locations on every line in the 39-bus system. In each case, the fault location is estimated over the time period 80-400 ms following the fault inception. Fault type identification is carried out to determine 1-ph-g faults for single-pole tripping of the faulted line. The real PMU model is used here for

TABLE I
PERFORMANCE OF THE PROPOSED WABP SCHEME WITH SYNCHRONIZED PHASOR MEASUREMENTS

Fault Resistance	0 Ω	10 Ω	50 Ω
FTISR* (%)	100	100	100
FLISR* (%)	99.7	99.5	99.0
FLE* (%)	0.63	0.65	0.81

* FTISR: Fault-type identification success rate; FLISR: Faulted-line identification success rate; FLE: Fault location error

phasor estimation because of its superiority in extracting phasors in non-ideal conditions compared to the DFT method. Obtained results are averaged and summarized in Table I in terms of fault-type identification success rate (FTISR), faulted-line identification success rate (FLISR), and fault location error (FLE). It can be seen that the proposed scheme successfully pinpoints the fault type and faulted line, irrespective of the fault resistance. In a very small number of cases the proposed scheme might mistake a neighboring line for the faulted line. Further simulations show that installing a PMU in the poorly observed areas will resolve this problem.

2) Advantages of using the Negative-Sequence Circuit:

To show the advantages of limiting the calculations to the assessment of the negative-sequence circuit, a solid 1-ph-g fault at 97.5% of line 25-26 is explored. Fig. 2 shows the *SoSR* of all transmission lines in both positive- and negative-sequence circuits. Within the first few cycles following the fault inception, the *SoSR* corresponding to the faulted line, i.e., the black dashed lines in Figs 2(a) and 2(b), take the smallest values amongst all. The negative-sequence *SoSR* remains quite small, no matter how long has passed since the fault inception. On the contrary, the positive-sequence *SoSR* steadily increases as time progresses and exceeds the *SoSR* of other lines around 150 ms after the fault inception. It becomes more likely to mistake a non-faulted line for the faulted one as more time progresses since the fault inception. This applies if calculations are carried out on the positive-sequence circuit and mainly for faults close to generator buses [9].

The faulted line may be still identifiable from the positive-sequence circuit by checking the fault distance estimated in that circuit. However, this solution might not be reliable, if the accuracy of the estimated fault distance deteriorates over time, similar to that of *SoSR*. To demonstrate this point, a solid 2-ph-g fault at 2.5% of line 22-23 is simulated. With reference to Figs 3(a) and 3(b), the estimated fault distance in the positive-sequence circuit loses its validity (contrary to that in the negative-sequence circuit) after approximately 100 ms following the fault inception. The oscillations of the estimated fault distance around its true value are more significant with DFT-estimated phasors than those with PMU outputs. This occurs since the interpolated-DFT algorithm implemented in the PMU model effectively overcomes the off-nominal frequency effects and the inclusion of decaying DC components in the input waveforms [34].

3) Faulted Line and Fault Type Identification:

The proposed scheme performs correctly regardless of CBs opening and their mode of opening (single-pole or three-pole mode). To demonstrate this capability, a solid 1-ph-g fault is considered at 5% of line 16-19. Fig. 4 shows the *SoSR* of all lines in the negative-sequence circuit, with the dotted line

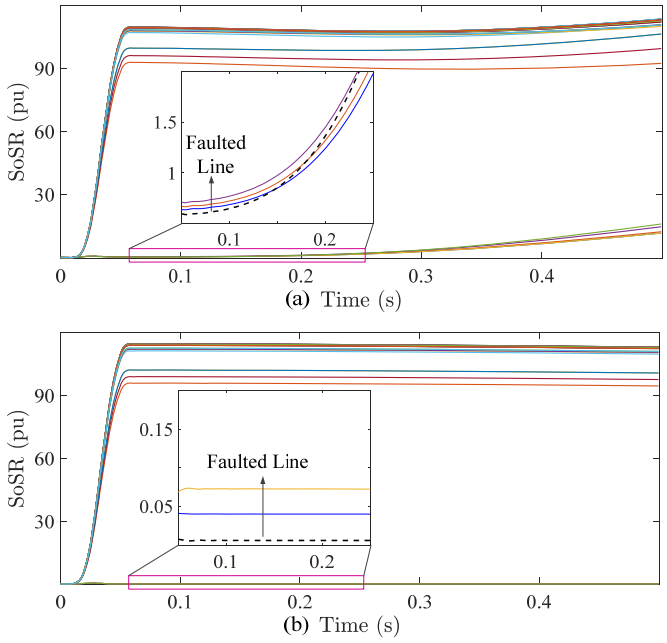

Fig. 2. (a) *SoSR* of transmission lines in the positive-sequence circuit, and (b) *SoSR* of transmission lines in the negative-sequence circuit.

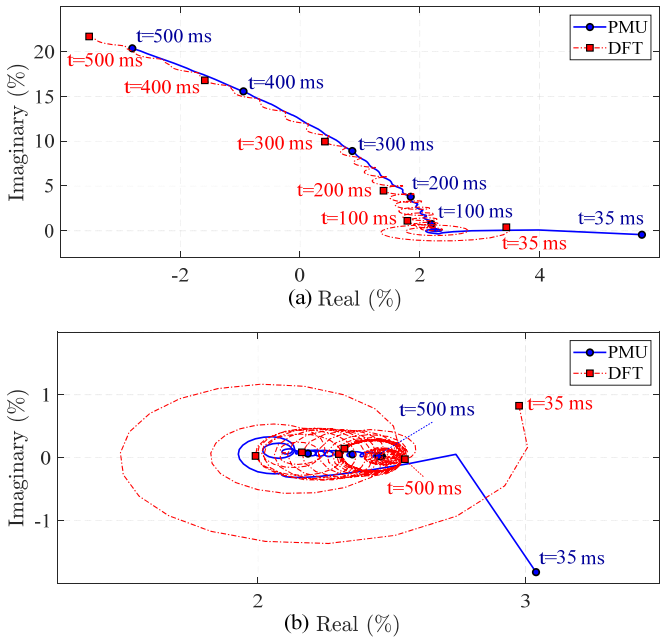

Fig. 3. Fault distance estimated over time for a 2-ph-g fault in (a) positive-sequence circuit, and (b) negative-sequence circuit.

being the *SoSR* of the faulted line. Let OSCB and ORCB denote the opening of the sending- and receiving-end CBs of the line, respectively. The OSCB and ORCB are set to occur 50 ms and 320 ms after the fault inception in both cases, respectively. It can be observed from Fig. 4 that the *SoSR* of the faulted line remains the smallest and the faulted line identification will not be affected by CBs opening. After the three-pole opening is completed from both line ends, the *SoSR* of all lines tends to become zero, since the negative-sequence circuit will not exist anymore once the system asymmetry is removed. It should be noted that the time between the fault inception and OSCB is 50 ms. Employing a 60-ms data window, the PMU model cannot provide fully reliable phasors

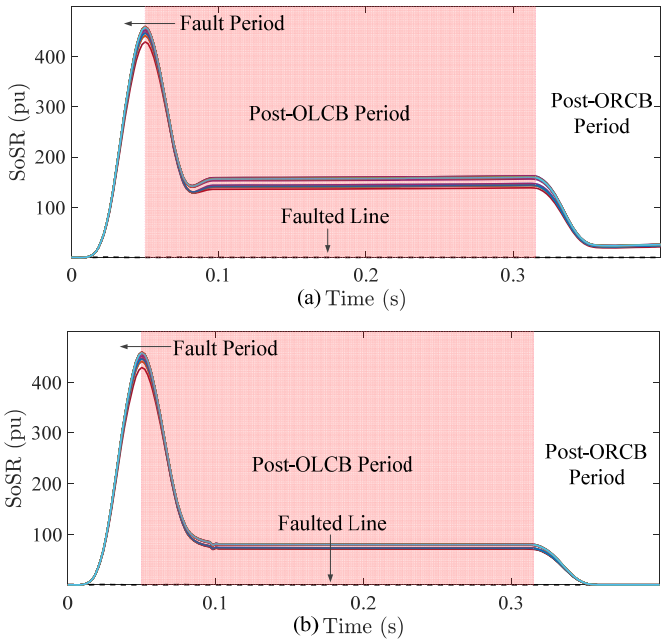

Fig. 4. *SoSR* of transmission lines in the negative-sequence circuit with (a) single-pole tripping enabled, (b) three-pole tripping enabled.

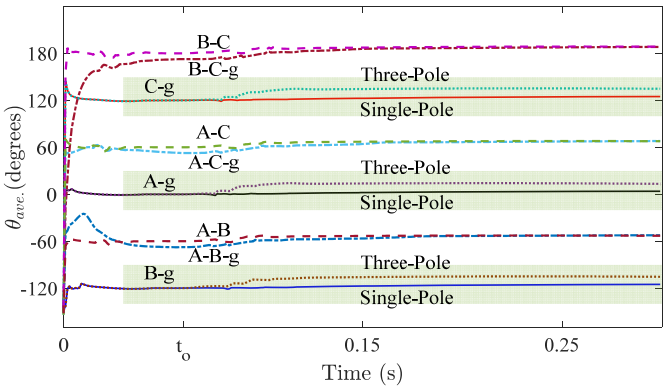

Fig. 5. Fault type identification for different types of fault with 10 Ω fault resistance at 5% of line 10-13 on the 39-bus test system.

estimation by this time. This could have created difficulties to the proposed WABP scheme, had the proposed scheme not been able to work with data of the post CB opening period.

The index proposed in (13) can effectively pinpoint 1-ph-g faults with no difficulties. For example, Fig. 5 shows the value of $\theta_{ave.}$ for different types of fault at 5% of line 10-13. It can be seen that the average angle difference $\theta_{ave.}$ remains in the specified range (green range) for all 1-ph-g faults and $\theta_{ave.}$ calculated in other fault types does not cause a malfunction. This has been verified to be the case for all simulated cases in the paper.

4) Backup Protection against Symmetrical Faults:

The proposed scheme is developed to provide backup protection against asymmetrical faults as the most frequent type of faults on transmission networks [3]. Nonetheless, the scheme can be also deployed for locating symmetrical (three-phase) faults with synchronized/unsynchronized input measurements. This can be achieved by replacing negative-sequence quantities with their positive-sequence counterparts in the formulations derived for backup protection against asymmetrical faults, i.e., (11) and (12). As an example, Fig. 6

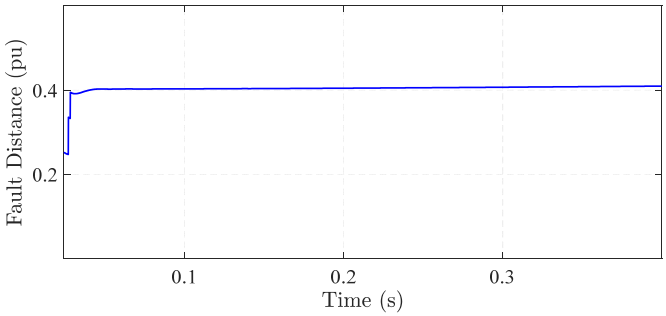

Fig. 6. Estimated fault distance for a three-phase fault at 40% of line 17-18.

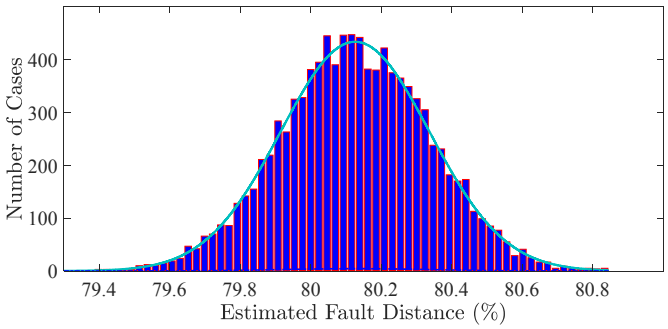

Fig. 7. Influence of phasor estimation errors on the fault location accuracy by unsynchronized measurements, for a 1-ph-g fault at 80% of line 6-7.

demonstrates the estimated fault distance over time for a three-phase fault at 40% of line 17-18.

Further simulations show that, with time, the imaginary part of the estimated fault distance in the positive-sequence circuit might gradually grow and its real part would further deviate from the actual fault distance. On the other hand, faulted line identification for symmetrical faults might not remain accurate for the same amount of time as that for asymmetrical faults. This applies to all WABP schemes that are based on the positive-sequence circuit to distinguish between the faulted and non-faulted transmission lines. For symmetrical faults, which do not involve the negative-sequence circuit, installing a few PMUs in the sparsely observed areas or a detailed modeling of generators can resolve the accuracy problem [9].

B. WABP using Unsynchronized Phasor Measurements

The ability of the proposed WABP scheme in functioning with unsynchronized phasors is demonstrated in this subsection. To make the inputs unsynchronized, phasors provided by each PMU is multiplied by a random complex number with a phase-angle between 0 and 2π. This complex number is selected so that it also accounts for a TVE of 1%.

Firstly, a solid 1-ph-g fault at 30% of line 6-7 is explored. For this arbitrarily selected case, estimated phasors are made unsynchronized as just described. This process is repeated 10000 times, and each time, the faulted line, fault type and fault distance on it are determined. Obtained results are depicted in Fig. 7. It can be observed that the error of estimated fault distances follows a normal distribution with a mean of 0.16 % and a standard deviation of 0.24 %.

Now, the entire simulations conducted in the previous subsection are repeated with unsynchronized measurements. Results shown in Table II confirm that the proposed scheme performs successfully even with unsynchronized input phasors. The average time needed for the identification of the

TABLE II
PERFORMANCE OF THE PROPOSED WABP SCHEME WITH UNSYNCHRONIZED PHASOR MEASUREMENTS

Fault Resistance	0 Ω	10 Ω	50 Ω
FTISR* (%)	100	100	100
FLISR* (%)	98.5	98.1	97.5
FLE* (%)	1.88	2.01	2.22

* FTISR: Fault-type identification success rate; FLISR: Faulted-line identification success rate; FLE: Fault location error

TABLE III
SENSITIVITY OF THE PROPOSED SCHEME TO LINE PARAMETER ERRORS

Results	Variation Range of Line Parameter Errors (%)									
	±1	±2	±3	±4	±5	±6	±7	±8	±9	±10
FLISR (%)	100	100	100	100	99.3	99.0	98.7	98.4	97.8	97.7
FLE (%)	0.76	0.90	1.09	1.14	1.55	1.68	1.78	2.11	2.23	2.39

TABLE IV
SENSITIVITY OF THE PROPOSED SCHEME TO MEASUREMENT ERRORS

Results	Variation Range of Measurement Errors (%)									
	±1	±2	±3	±4	±5	±6	±7	±8	±9	±10
FLISR (%)	100	100	100	100	99.9	99.7	99.6	99.3	98.7	98.4
FLE (%)	0.73	0.82	0.91	1.04	1.20	1.25	1.40	1.62	1.75	1.93

faulted line with unsynchronized measurements is calculated to be around 20 ms. This time is quite negligible, compared to communication delays involved in wide-area applications. This average execution time is essentially an upper bound, for not taking into account the possibility of parallel computation at software and/or hardware levels. Indeed, the *SoSR* calculations are completely independent for different lines. Therefore, the proposed WABP scheme could be highly parallelized, so that the whole execution time drops down to a few milliseconds or less.

C. Sensitivity to Measurement and Line Parameter Errors

WABP is mainly concerned with the identification of the faulted line rather than pinpointing the exact fault location on the faulted line. It is shown in this subsection that the former, is not as much sensitive to measurement or line parameter errors. Firstly, an extensive number of simulations are conducted to study the effect of transmission line parameter errors on the success rate of faulted-line identification by the scheme. Table III provides the results with random parameter errors within different ranges for faults at 50 different locations on all transmission lines. It can be seen that up to 4% of line parameter errors, the proposed WABP scheme remains successful in faulted line identification. As expected, the success rate of the scheme decreases as the variation range of line parameter errors increases.

The success rate of the proposed scheme, similar to that of any other scheme, is also dependent on measurement errors. A number of faults are applied at 50 different locations on all transmission lines to demonstrate the effect of measurement errors greater than 1% TVE (set out by the standard), on the success rate. Measurement errors are assumed to have a normal distribution around the true value of corresponding phasors. The fault resistance is 10 Ω in this study. Table IV tabulates obtained results where the three-sigma criterion is used for reporting the error range [9]. As expected, larger measurement errors result in less success rate for the proposed scheme. From a practical point of view, however, the low-demanding scheme proposed can be used to provide backup protection against short-circuit faults.

TABLE V
PERFORMANCE COMPARISON BETWEEN DIFFERENT WABP SCHEMES

Comparison aspect	[12] and [18-26]	[13-16]	[28]	Proposed
Single/Multiple Loss of PMUs	Intolerant	Tolerant	Tolerant	Tolerant
Need Time-Synch Signal?	Yes	Yes	No	No
Involve Iterative Solution?	No	No	Yes	No
Specific PMU Placement?	Yes	No	No	No
Identification of 1-ph-g faults?	No	No	No	Yes
Accurate over time?	No	No	No	Yes
Computation time	Low	Low	High	Low

D. Comparison with Existing WABP Schemes

Table V compares the proposed WABP scheme with its existing counterparts and the wide-area fault location methods that can be used for this purpose. As can be seen, the proposed scheme delivers better performance than the existing schemes. The majority of the existing schemes require synchrophasors and consequently are sensitive to time-synchronization errors. Only the scheme presented in [28] can take advantage of hybrid synchronized/unsynchronized phasor measurements as inputs. Nonetheless, this scheme is computationally demanding, considering its need for iterative methods to solve a system of non-linear equations.

The WABP schemes proposed in [12] and [18-26] are unable to identify the faulted line by an arbitrary set of PMUs unless specific constraints are met by PMU locations. The loss of time-synchronization signal prevents all these schemes from functioning properly. The new scheme proposed in this paper is the only one that can correctly pinpoint the faulted line for over hundreds of milliseconds. Input phasors to this scheme do not require to be time-synchronized, which significantly contributes to the robustness and reliability of protection it provides. The scheme is also capable of fault type identification, which is a prerequisite for single-pole tripping of CBs [1].

IV. CONCLUSIONS

In this paper, a novel wide-area backup protection (WABP) scheme is proposed for asymmetrical faults on transmission systems, using available synchronized/unsynchronized phasor measurements. The proposed scheme can identify the faulted line and retain this capability for over hundreds of milliseconds following a fault inception. This enables establishing an effective two-way communication between the wide-area and local protection systems until the fault is cleared. The scheme can also easily identify single-phase-to-ground (1-ph-g) faults, facilitating single-pole opening of circuit breakers, if recommended for improving overall system stability. The linearity of the formulations derived not only removes concerns over convergence speed and/or multiplicity of the solution, but also facilitates overcoming the presence of synchronization errors or a complete loss of the time-synchronization signal.

The above-mentioned advantages are beyond the capabilities of existing WABP schemes and can be simply achieved by restricting the fault calculations to the assessment of the negative-sequence circuit of the grid. This technique is justified through rigorous analytical discussions and simulation studies. The speed of backup protection is becoming increasingly important in modern power systems with volatile/reduced system inertia. The scheme lends itself to practical real-time applications thanks to its low-demanding nature in terms of computational burden and limited input data it requires. The idea of using only negative-sequence circuit can be also extended in the future to monitoring and dealing with other asymmetrical events. This includes but is not limited to single-pole tripping and reclosing of transmission lines, which can significantly contribute to secure operation of power systems.

REFERENCES

[1] P. M. Anderson, *Power System Protection*. New York: IEEE Press, 1999.

[2] S. H. Horowitz and A. G. Phadke, *Power System Relaying*, 3rd ed. John Wiley & Sons, 2008.

[3] N. D. Tleis, *Power Systems Modeling and Fault Analysis: Theory and Practice*. 7th ed., Oxford, UK: Newnes, 2008.

[4] M. M. Saha, J. J. Izykowski, and E. Rosolowski, *Fault Location on Power Networks*, 1st ed., Springer: London, 2010.

[5] S. A. N. Sarmadi, A. S. Dobakhshari, S. Azizi, A. M. Ranjbar and S. Nourizadeh, "A sectionalizing method in power system restoration based on Wide Area Measurement Systems," *2010 IEEE Electrical Power & Energy Conference*, Halifax, NS, 2010, pp. 1-6.

[6] W. A. Elmore, *Protective Relaying: Theory and Applications*, CRC, Press, 2003.

[7] J. L. Blackburn and T. J. Domin, *Protective Relaying: Principles and Applications*, CRC Press, 2014.

[8] G. Ziegler, *Numerical Distance Protection: Principles and Applications*, 4th ed. 2011.

[9] S. Azizi and M. Sanaye-Pasand, "From available synchrophasor data to short-circuit fault identity: Formulation and feasibility analysis," *IEEE Trans. Power Syst*., vol. 32, no. 3, pp. 2062-2071, May 2017.

[10] ALSTOM, *Network Protection and Automation Guide*, *2002*.

[11] V. Terzija *et al.*, "Wide-area monitoring, protection, and control of future electric power networks," *Proc. IEEE*, vol. 99, no. 1, pp. 80–93, Jan. 2011.

[12] A. Sharafi, M. Sanaye-Pasand, and F. Aminifar, "Transmission system wide-area back-up protection using current phasor measurements," *International Journal of Electrical Power & Energy Systems*, vol. 92, pp. 93-103, Nov. 2017.

[13] S. Azizi and M. Sanaye-Pasand, "A straightforward method for wide-area fault location on transmission networks," *IEEE Trans. on Power Del.*, vol. 30, no. 1, pp. 264-272, Feb. 2015.

[14] Y. Liao, "Fault location for single-circuit line based on bus-impedance matrix utilizing voltage measurements," *IEEE Trans. Power Del.,* vol. 23, no. 2, pp. 609–617, Apr. 2008.

[15] M. Majidi, M. Etezadi-Amoli, M. S. Fadali, "A sparse-data-driven approach for fault location in transmission networks," *IEEE Trans. Smart Grid*, vol. 8, no. 2, pp. 548-556, Mar. 2017.

[16] S. Azizi, M. Sanaye-Pasand, and M. Paolone, "Locating faults on untransposed, meshed transmission networks using a limited number of synchrophasor measurements," *IEEE Trans. Power Syst.*, vol. 31, no. 6, pp. 4462-4472, Nov. 2016.

[17] R. Giovanini, K. Hopkinson, D. V. Coury, and J. S. Thorp, "A primary and backup cooperative protection system based on wide area agents," *IEEE Trans. Power Del*., vol. 21, no. 3, pp. 1222–1230, Jul. 2006.

[18] S. Garlapati, H. Lin, A. Heier, S. K. Shukla, and J. Thorp, "A hierarchically distributed non-intrusive agent aided distance relaying protection scheme to supervise zone 3," *Elect. Power Energy Sys*t., vol. 50, pp. 42–49, Sep. 2013.

[19] Z. He, Z. Zhang, W. Chen, O. P. Malik, and X. Yin, "Wide-area backup protection algorithm based on fault component voltage distribution," *IEEE Trans. Power Del.,* vol. 26, no. 4, pp. 2752–2760, Oct. 2011.

[20] J. Ma *et al*., "A fault steady state component-based wide area backup protection algorithm," *IEEE Trans. Smart Grid,* vol. 2, no. 3, pp. 468–475, Sep. 2011.

[21] H. K. Zadeh and Z. Li, "Phasor measurement unit-based transmission line protection scheme design," *Elect. Power Syst. Res.,* vol. 81, no. 2, pp. 421–429, Feb. 2011.

[22] P. Kundu, A. K. Pradhan. "Synchrophasor-assisted zone-3 operation." *IEEE Trans. Power Syst.*, vol. 29, no. 2, pp. 660–667, Apr. 2014.

[23] P. V. Navalkar, S. A. Soman. "Secure remote backup protection of transmission lines using synchrophasors." *IEEE Trans. Power Del.,* vol. 26, no. 1, pp. 87–96, Jul. 2011.

[24] J. Zare, F. Aminifar, M. Sanaye-Pasand, "Synchrophasor-based wide-area backup protection scheme with data requirement analysis." *IEEE Trans. Power Del.,* vol. 30, no. 3, pp. 1410–1419, Jun. 2015.

[25] J. Ma *et al*., "A wide-area backup protection algorithm based on distance protection fitting factor." *IEEE Trans. Power Del.,* vol. 31, no. 5, pp. 2196–2205, Oct. 2016.

[26] M. K. Neyestanaki and A. M. Ranjbar, "An adaptive PMU-based wide area backup protection scheme for power transmission lines," *IEEE Trans. Smart Grid*, vol. 6, no. 3, pp. 1550–1559, May 2015.

[27] Z. H. Rather, Z. Chen, P. Thøgersen, P. Lund, and B. Kirby, "Realistic approach for phasor measurement unit placement: Consideration of practical hidden costs," *IEEE Trans. Power Del.*, vol. 30, no. 1, pp. 3–15, Feb. 2015.

[28] A. S. Dobakhshari, "Wide-area fault location of transmission lines by hybrid synchronized/unsynchronized voltage measurements," *IEEE Trans. Smart Grid*, vol. 9, no. 3, pp. 1869–1877, May 2018.

[29] C. A. Desoer and E. S. Kuh, *Basic Circuit Theory*, New Delhi: Tata McGraw-Hill, 2009.

[30] W. Yao, *et al.*, "Impact of GPS signal loss and its mitigation in power system synchronized measurement devices," *IEEE Trans. Smart Grid*, vol. 9, no. 2, pp. 1141-1149, Mar. 2016.

[31] *IEEE Standard for Synchrophasor Measurements for Power Systems*, IEEE Std. C37.118.1-2011, 2011.

[32] R. D. Zimmerman, C. E. Murillo-Sanchez, and D. Gan, "Matpower, a MATLAB Power System Simulation Package". ver. 3.2, 2007. [Online]. Available: http://www.pserc.cornell.edu/matpower/.

[33] S. Azizi, A. S. Dobakhshari, S. A. N. Sarmadi, and A. M. Ranjbar, "Optimal PMU placement by an equivalent linear formulation for exhaustive search," *IEEE Trans. Smart Grid*, vol. 3, no. 1, pp. 174–182, Mar. 2012.

[34] P. Romano, and M. Paolone, "Enhanced interpolated-DFT for synchrophasor estimation in FPGAs: Theory, implementation, and validation of a PMU prototype," *IEEE Trans. Instrum. Meas*., vol. 63, no. 12, pp. 2824–2836, Dec. 2014.